An EEG-based attentiveness recognition system using Hilbert-Huang transform and support vector machine

Chia-Ju Peng, Yi-Chun Chen, Chun-Chuan Chen, Shih-Jui Chen, Barthelemy Cagneau, Luc Chassagne

An EEG-based attentiveness recognition system using Hilbert-Huang transform and support vector machine

Chia-Ju Peng[1,4], Yi-Chun Chen[2], Chun-Chuan Chen[3], Shih-Jui Chen[1,*], Barthélemy Cagneau[4], and Luc Chassagne[4]

[1]Department of Mechanical Engineering, National Central University, Taoyuan, Taiwan
[2]Department of Optics and Photonics, National Central University, Taoyuan, Taiwan
[3]Department of Biomedical Sciences and Engineering, National Central University, Taoyuan, Taiwan
[4]Laboratoire d'Ingénierie des Systèmes de Versailles, Université de Versailles Saint-Quentin en Yvelines, Vélizy, France

[*]Corresponding author: E-mail: raychen@cc.ncu.edu.tw

Hilbert-Huang transform (HHT) is useful for the analysis of nonlinear or nonstationary bio-signals including brainwaves. In this work, a method is proposed for the characterization of the levels of attentiveness by using electroencephalogram (EEG) signals and HHT analysis. Single channel EEG signals over the frontal area were acquired from participants at different levels of attentiveness and were decomposed into a set of intrinsic mode functions (IMF) by empirical mode decomposition (EMD). Hilbert transform analysis was applied to each IMF to obtain the marginal frequency spectra, and then the band powers and spectral entropies (SE) were selected as the attributes entered a support vector machine (SVM) for the two-class classification. Compared with the predictive models of approximate entropy (ApEn) and fast Fourier transform (FFT), the results showed that the band powers extracted from IMF2 to IMF5 of α and β waves and their SE can best discriminate between attentive and relaxed states with the classification average accuracy of 84.80%. In conclusion, this integrated signal processing method is capable of attentiveness recognition and may be used in a clinical setting for the detection of attention deficit.

1. Introduction

Attention is an important feature that reflects the mental state of the brain and can be measured by using electroencephalography (EEG). The measurement of the degree of attention is mainly associated with α and β waves [1]. In particular, α waves between 8 and 13 Hz with amplitudes from 30 to 50 μV are evident on the EEG of a relaxed participant with closed eyes. The β oscillations between 14 and 30 Hz with amplitudes from 5 to 20 μV are evident during active attention. Therefore, quantifying these frequency-specific features using EEG can be used to probe the level of attentiveness [2,3].

Previous studies have shown that for EEG attentiveness recognition, using a k-nearest neighbor classifier based on the self-assessment manikin model can yield an average accuracy of 57.03% [4], and using support vector machine (SVM) model of power spectral density resulted in an average accuracy of 76.82% [5]. In addition, the accuracy can be increased to 81% when taking into account approximate entropy using fuzzy entropy [6]. On a single subject level, the accuracy is up to 89.4% when using the integration of common spatial pattern filtering and nonlinear mutual information method [7]. Taken together, frequency-specific and nonlinear features extracted from EEG are essential for attentiveness recognition. Therefore, in this study, we proposed a method for the characterization of the levels of attentiveness based on Hilbert-Huang transform (HHT) and SVM. HHT has been used to process nonlinear and nonstationary brainwave signals [8,9] in EEG analysis and clinical applications, such as motor imaginary [10], seizure detection [11-13], and anesthesia monitoring [14,15]. SVM, a machine learning technique, gradually becomes a popular translation method for classification with high accuracy [16-18]. Given a set of training samples, SVM can build a predictive model of the specific EEG features by the supervised learning algorithm, performing a classifier for attentiveness.

In this study, we measured the brain activity over the frontal area with one channel EEG

device during participants solving some puzzles shown on the screen as well as during a resting period. EEG signals were first decomposed to intrinsic mode functions (IMF) using empirical mode decomposition (EMD), after which the instantaneous frequencies of IMFs were obtained using HHT. The resulting marginal spectra (MS) of specific frequency bands and spectral entropy (SE) entered an SVM as the feature attributes for characterization of attentiveness.

2. Materials and methods

2-1. Data collection

EEG data were measured by using a commercial mobile EEG monitor (MindWave, *NeuroSky*) at a sampling rate of 512 Hz [19]. The unipolar recording device had a fixed channel position on the scalp surface of the forehead (Fp1), according to the International 10/20 system [20]. An ear clip (A1) of the device was used to provide a ground reference to filter out the electrical noise.

This study, numbered 201812EM027, was approved by the Research Ethics Committee of National Taiwan University, Taiwan. Twenty participants were recruited: eight males and twelve females, whose ages ranged from 20 to 26 (average age = 21.9). The participants were instructed to sit still in a quiet room, wearing the EEG monitor. Two tasks were conducted by the participants: (1) pay their attention on solving designated spot-the-difference puzzles shown on a screen for 5 minutes; (2) then relax with their eyes opened and fixated at a blank screen for 5 minutes. Figure 1 shows the EEG of a representative participant during the two tasks. The dashed lines indicate the onset of the rest task. The continuous EEG signal was epoched as a collection of time-locked trials with the time length of 1 second. The middle 200 epochs of each task were analyzed to build a classifying model. As shown in Figure 1, the red block is considered as attention data (200 epochs), and the

green block is relaxation data (200 epochs). Therefore, 200 attention and 200 relaxation epochs of twenty participants were analyzed to build the individualized classifiers. Besides, both of the last 50 epochs were used as the testing data to validate the models. The flowchart of this study is shown in Figure 2. The selected features of EEG data extracted by Hilbert-Huang analysis (EMD, HT, and MS) were entered the SVM for attentiveness recognition.

2-2. Hilbert-Huang Transform

HHT [21] is a time–frequency–energy method for the analysis of nonlinear or non-stationary data sets, the process of which can be divided into two parts: EMD and the Hilbert transform (HT) [22]. For dealing with nonlinear and non-stationary signals and extracting the basis for the HT, EMD has been proposed to generate finite component sets empirically from original data. The repetitive extraction of EMD is based on the oscillatory modes and waveforms of signals in the time domain, assuming that any data comprises different simple intrinsic oscillatory modes. An IMF of a signal is a function with (1) the same number of zero-crossings and extrema, and with (2) symmetric envelopes defined by local maxima and minima. Meeting these conditions, IMFs form an orthogonal basis for the original signal. The definition guarantees the HT of IMF has well behavior to analyze the instantaneous frequency benefited from its simple oscillation. The procedure of extracting an IMF is called the sifting process of EMD, which is used to remove riding waves and symmetrize the wave profiles. The sifting process should be repeated as many times as necessary to convert the extracted signal into an IMF. Thus, a signal, $x(t)$, can be represented as

$$x(t) = \sum_{i=1}^{n} c_i(t) + r_n(t), \quad (1)$$

where $c_i(t)$ and $r_n(t)$ are the i^{th} IMF and the residue, respectively [10,21]. All raw EEG epochs in this study were decomposed into 8 IMFs and a residue, the number of which was determined by sample length and stopping criteria of the sifting process.

After the EMD process, the HT of the i^{th} IMF can be calculated as [23]

$$y_i(t) = \frac{1}{\pi} P \int_{-\infty}^{\infty} \frac{c_i(\tau)}{t-\tau} d\tau, \quad (2)$$

where P is the Cauchy principal value. By arranging $c_i(t)$ and $y_i(t)$ into a complex pair, an analytic signal $z_i(t)$ can be formed as

$$z_i(t) = a_i(t)\mathrm{e}^{j\emptyset_i(t)} = c_i(t) + jy_i(t), \quad (3)$$

where $a_i(t)$ is defined as the instantaneous amplitude, and $\emptyset_i(t)$ is defined as the instantaneous phase. Hence all HT of IMFs constitute the HHT spectrum $H(\omega, t)$ of whole signal $x(t)$, presenting time-frequency-energy information as a 3D spectrum:

$$H(\omega, t) = HHT\{x(t)\} = \sum_{i=1}^{n} a_i(t) e^{j\int \omega_i(t)dt}, \quad (4)$$

where $\omega_i(t)$ is defined as instantaneous angular frequency as $d\emptyset_i(t)/dt$, and the residue $r_n(t)$ is omitted. Finally, the MS, representing the accumulated energy over the entire data span from the contribution of each frequency value, can be defined as:

$$h(\omega) = \int_0^T H(\omega, t)dt. \quad (5)$$

Moreover, SE was further used to measure the quantities of signal disorder in the frequency domain [24], and SE can be evaluated by the normalized powers of frequencies:

$$\mathrm{SE} = -\frac{\sum_f \left(\hat{h}(f) \log_2 \hat{h}(f)\right)}{\log_2 m}, \quad (6)$$

where $\hat{h}(f) = \frac{h(f)}{\sum h(f)}$ is the normalized frequency component and m is the number of frequency components. The normalized entropy values were between 0 (complete regularity) and 1 (maximum irregularity), showing the concentration of frequency distribution [25].

2-3. Feature selection and Support vector machine

Having extracted the frequency-specific power from HHT and computed the SE, we employed the linear forward selection method to reduce the number of attributes that enter

SVM.

The SVM was developed from statistical learning theory to analyze a data set for the classification of multi-classes [26,27]. A data set is trained to acquire a mathematical model, which is used to discriminate a testing data set. For binary classification, an SVM model constructs a hyperplane that optimally separates data sets into one of two classes, and the distance from the hyperplane to the nearest data points on each side is maximized.

Assuming the testing data set is linearly separable, a general form of hyperplane can be defined by $\mathbf{w}^{\mathrm{T}}\mathbf{x} + \mathrm{b} = 0$, where $\mathbf{w}$ is the normal vector to the hyperplane, and b is the bias term, and a classifier, $d = \mathrm{sgn}(\mathbf{w}^{\mathrm{T}}\mathbf{x} + \mathrm{b})$, can be selected. For each data point $\mathbf{x}_i$, the following equation must be satisfied:

$$d_i(\mathbf{w}^{\mathrm{T}}\mathbf{x}_i + \mathrm{b}) \geq 1, \text{for } 1 \leq i \leq n. \tag{7}$$

$\mathbf{w}$ and b are then optimized to set an optimal separating hyperplane, and the margin between the two classes is maximized [26].

If the testing data set is not linearly separable, slack variables ξ_i are introduced to measure the degree of misclassification, and the primal problem is modified to [27]

$$\begin{aligned} &\text{minimize: } \|\mathbf{w}\|^2/2 + C\sum \xi_i \\ &\text{subject to: } d_i(\mathbf{w}^{\mathrm{T}}\boldsymbol{\Phi}(\mathbf{x}_i) + \mathrm{b}) \geq 1 - \xi_i, \text{for } 1 \leq i \leq n, \end{aligned} \tag{8}$$

where C is the regularization parameter, which controls the punishment for misclassified data points and $\boldsymbol{\Phi}(\mathbf{x}_i)$ maps $\mathbf{x}_i$ into a higher dimensional space to make the separation in that space easier. To reduce the computational load, the Representer Theorem [28] shows that $\mathbf{w}$ with large dimensionality can be written as a linear combination of the training data, $\mathbf{w} = \sum \alpha_i d_i \boldsymbol{\Phi}(\mathbf{x}_i)$. Therefore, we can optimize α_i instead of $\mathbf{w}$, and the decision function becomes

$$f(\mathbf{x}) = \sum \alpha_i d_i K(\mathbf{x}_i, \mathbf{x}) + \mathrm{b}, \tag{9}$$

where $K(\mathbf{x}_i, \mathbf{x}) = \mathbf{\Phi}(\mathbf{x}_i)^{\mathrm{T}}\mathbf{\Phi}(\mathbf{x})$ is the kernel function. The new dual problem is modified to [29]:

maximize: $\sum_i \alpha_i - 1/2 \times \sum_{jk} \alpha_j \alpha_k d_j d_k K(\mathbf{x}_j, \mathbf{x}_k)$

subject to: $0 \leq \alpha_i \leq C, and \ \sum_i \alpha_i d_i = 0.$ (10)

In this study, a Gaussian radial basis function (RBF) kernel, $K(\mathbf{x}, \mathbf{x}') = \exp(-\gamma\|\mathbf{x} - \mathbf{x}'\|^2)$, was used. Both C and γ are carefully chosen to obtain optimal results.

A typical procedure of LIBSVM [27] involves several steps: (1) the input of attributes of a data set with pre-classified indices, (2) training the data to build a model, and (3) predicting the classification or information of a test data set from the model. In the c-support vector classification in this study, the attribute vectors of attention epochs were labeled as class 1 in advance, while those of relaxed epochs were labeled as class -1. These attribute vectors with two-task labels comprised an input matrix for SVM training. After building the models, the classification of new epochs can be predicted using these models.

3. Results and discussions

Figure 3 presents the full HHT 3D spectrum of the signal in Figure 1, providing the time-frequency-energy distribution of the continuous data in one trial. One of the participants paid attention for 300 seconds and then relaxed. The high energy located in a low-frequency band may include artifacts such as blinks. It is noted that the energy of high frequencies in the red block is statistically larger than which in the green block, indicating that the alpha and beta waves are indeed different in attention/inattention task ($T=4.4049$, $p<0.05$).

The raw signals and their IMFs of an attention epoch and a relaxation epoch are presented in Figure 4 (a) and (b), respectively. 8 IMFs and a residual trend of the epoch were extracted by EMD. After performing the Hilbert transform, we found that IMF2, IMF3,

IMF4, and IMF5 contained the power within the desired frequency range (8~30 Hz) while the IMF1, IMF6~8 contained statistically no power in the frequencies of interest ($p<0.05$). The marginal spectrum of an IMF presents the time integration of its 3D spectrum and describes the distribution of power contained in the IMF as a function of frequency. Figure 5 shows the marginal spectra of IMF2 to IMF5, which were used to derive the features of frequency.

Table I lists the attention assessment results of a representative participant using SVM with several attribute vectors. Regarding the impact of attributes on the accuracy, the features comprising of α and β powers estimated from {IMF2~IMF5 and SE} #6 obtained the best classification result of 93.25% accuracy. Frequency-specific power attributes of the original EEG signal after HHT {α-original, β-original} #1 resulted in 85.25% accuracy, suggesting an essential role in reflecting the attentiveness. The result that {SE} #4 feature alone could obtain the prediction accuracy of 86.25% suggested that the nonlinear characteristics of brain dynamics were important indicators of the mental states. Table I also indicates that using more features as the attributes did not help to obtain better accuracy. The result of feature selection of machine learning further confirmed that IMF1 and IMF6~IMF8 were not important features for classification. In other words, the most important EEG features that can reflect the state of attentiveness in this study are the attributes #6: α-IMF2, α-IMF3, α-IMF4, α-IMF5, β-IMF2, β-IMF3, β-IMF4, β-IMF5, α-SE, and β-SE.

Having established the individualized predictive models of SVM, we tested the predictive model to classify the attentiveness state of each participant as listed in Table II. The mean self-accuracy of 84.80% with 10-fold cross validation shows that the selected features can offer efficient differentiation for the assessment of attentiveness. To validate the individualized models that we built, additional 50 attention and 50 relaxation epochs of

each participant were treated as the independent test data. The models classified the test data and outputted the predictions of the attentiveness, the accuracy of which are listed in Table III. The results show the agreement of the predictive models.

To compare with the proposed method that generated the time-frequency-domain and nonlinear features, we also implemented two analytic methods: the approximate entropy (ApEn) of original EEG signal as a time-domain and nonlinear feature, and the power spectral density of original EEG signal estimated by fast Fourier transform (FFT) as a frequency-domain and linear feature. These features were then respectively input into SVM as the attributes to build the predictive models for comparison. Figure 6 presents the boxplots of the above three methods, and the one-way ANOVA indicates the statistically significant differences in their results ($p < 0.01$). The SVM model of ApEn had a mean accuracy 73.94% with the smallest standard deviation compared to the others. The SVM model of FFT had a mean accuracy 77.80%, however, its large standard deviation indicated that there was huge between-subject variability in FFT features. According to the results, the proposed method of SVM combining with HHT can best discriminate between attentive and relaxed states.

Moreover, in this method, we used only one channel data to build the predictive models and yielded good accuracy up to 96.00% with an average of twenty participants being 83.90%. EEG recording using more channels may help improve the system; nevertheless, the single channel EEG monitor is inexpensive, convenient and portable for publics. We believe that this convenient method has the potential to be used in clinical settings for the detection of attention deficit.

4. Conclusion

A method of feature extraction and characterization of EEG signals using HHT

frequency analysis and SVM has been presented. Raw EEG data have been analyzed by HHT to obtain marginal spectra for nonlinear and nonstationary frequency information. The α and β band powers of IMF2~5 and their spectral entropies were selected as the attributes of SVM to obtain the mean accuracy of 84.80%. We conclude that the proposed method can offer efficient differentiation for the assessment of attentiveness, showing promise in applications of attention deficit detection or biofeedback training.

Acknowledgments

This material is based upon work supported by the Ministry of Science and Technology, Taiwan, under contract no. MOST 106-2221-E-008-042, MOST 106-2221-E-008-066-MY2 and MOST 105-2221-E-008-038.

Competing interests: The authors declare that they have no conflict of interest.

Funding: Ministry of Science and Technology, Taiwan

Ethical approval: This study, numbered 201812EM027, was approved by the Research Ethics Committee of National Taiwan University, Taiwan.

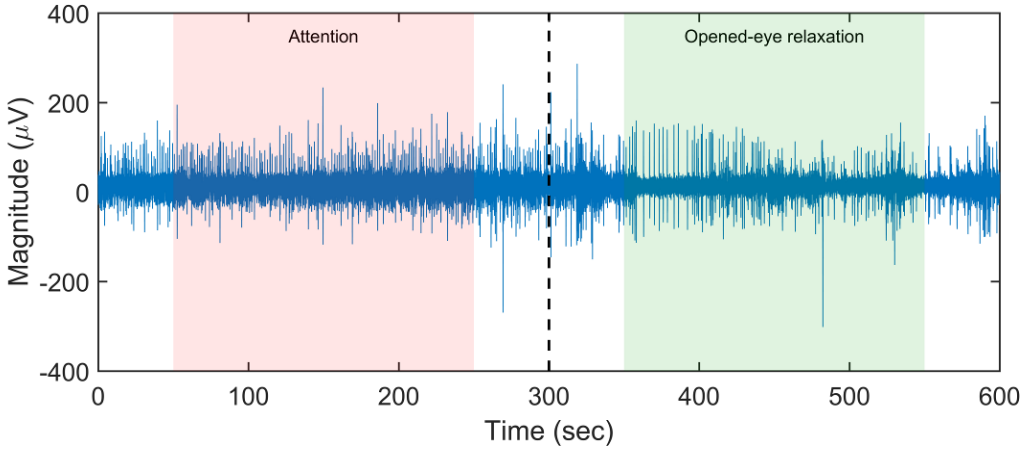

Figure 1. A continuous raw EEG signal of a representative participant while conducting two tasks. The participant paid attention for 5 minutes (until the dotted line) and then took a break with eyes opened for another 5 minutes. The epochs in the red block were collected as attention data, and the epochs in the green block were collected as relaxation data for further analysis.

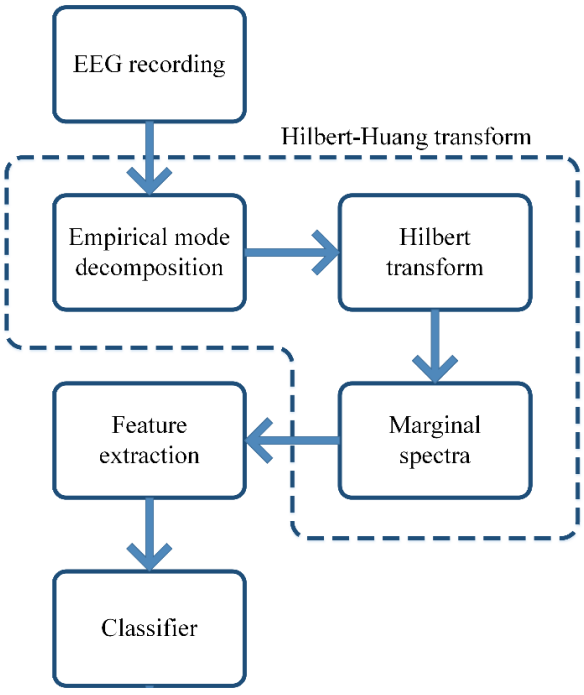

Figure 2. The flowchart of the proposed method. The EEG data were treated with Hilbert-Huang analysis to obtain the time-frequency information. The extracted features were the input of the support vector machine to build a proper classifier for attentiveness recognition.

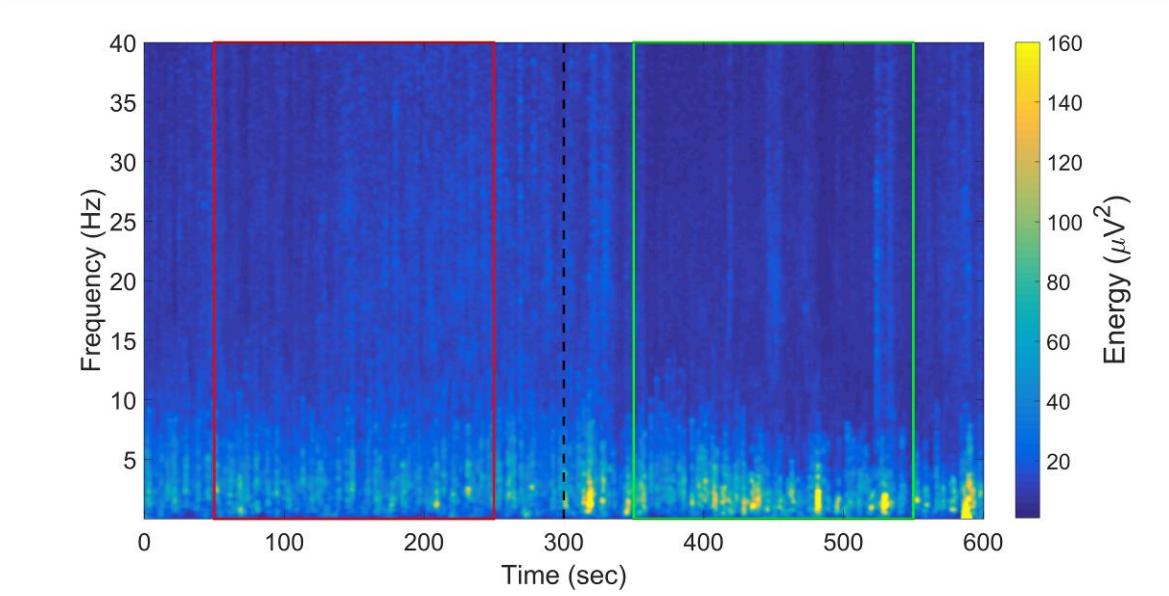

Figure 3. The HHT spectrum of the representative participant while conducting two tasks. The colorbar shows the magnitude of the energy distribution. The conducted task was switched at the 300th second. The time-frequency-energy information of attentive and relaxed tasks are illustrated in red and green blocks, respectively.

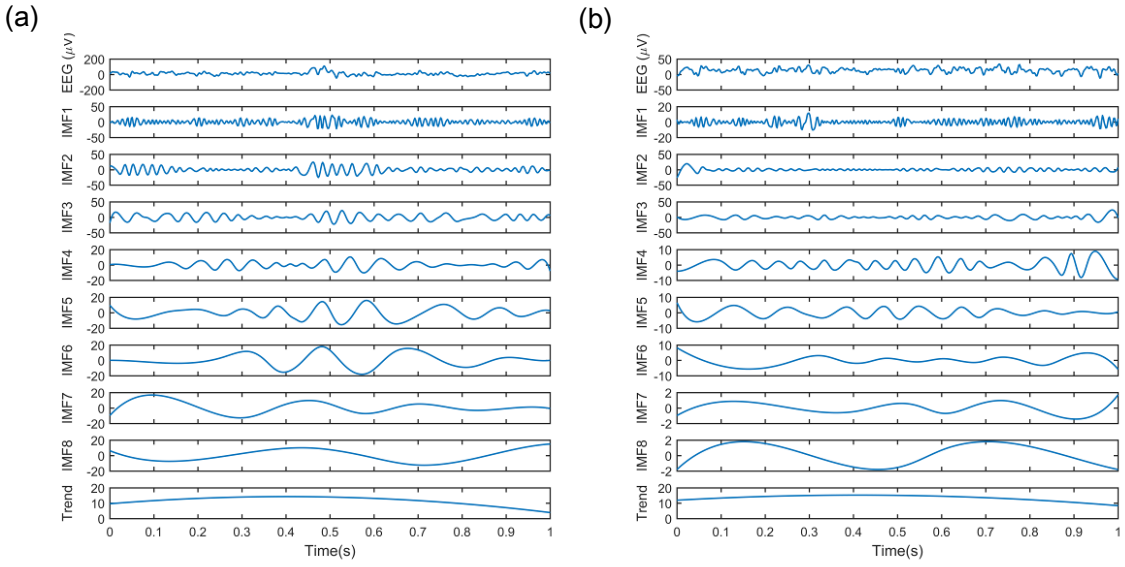

Figure 4. (a) IMFs of an EEG epoch when the representative participant was paying attention to solve a puzzle. (b) IMFs of an EEG epoch when the representative participant had been instructed to relax and take a rest.

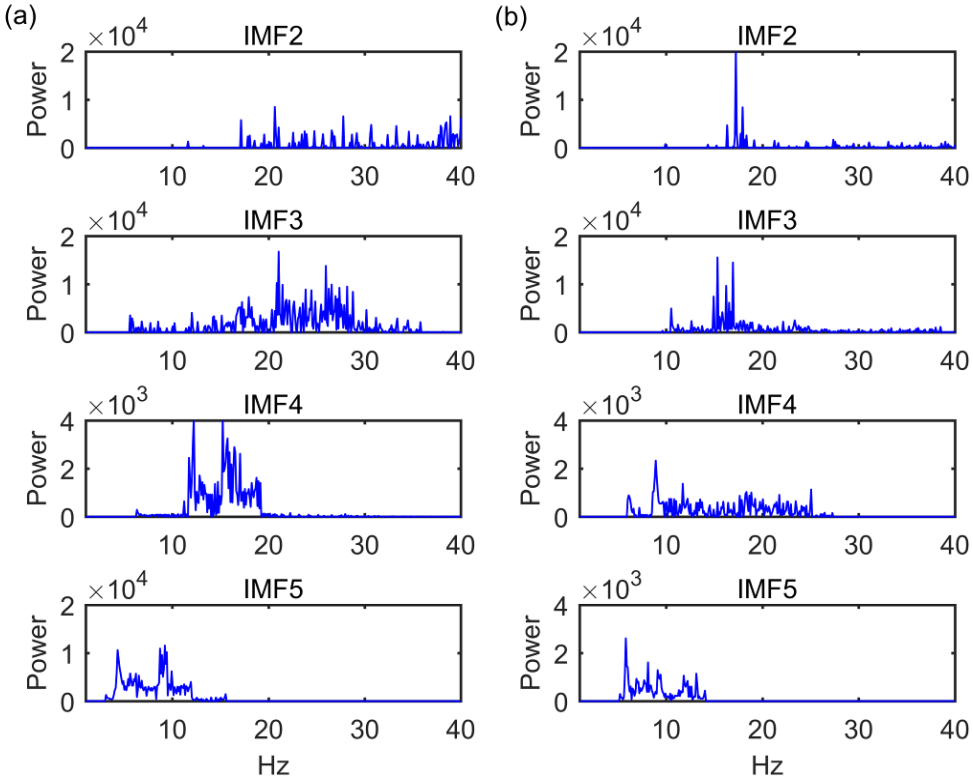

Figure 5. Marginal spectra of IMF2~5 when the representative participant was (a) paying attention and (b) taking a rest.

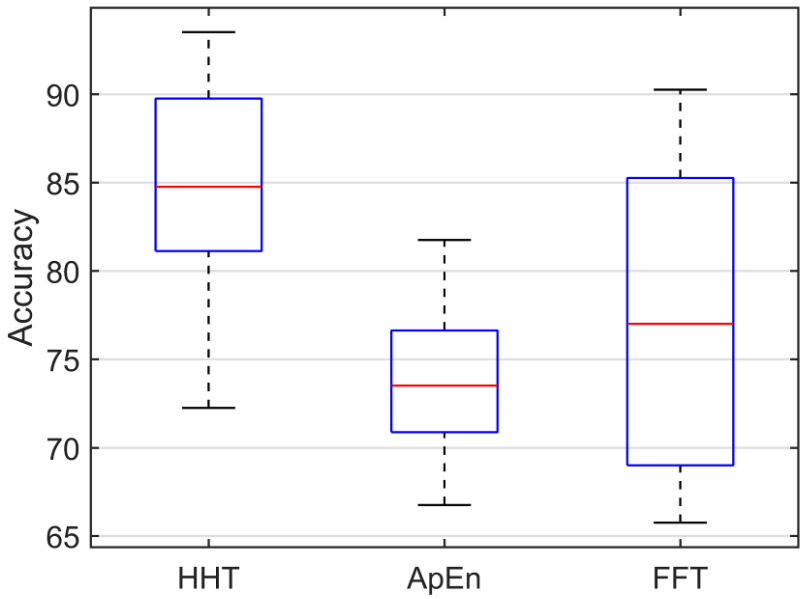

Figure 6. The boxplots of accuracy of SVM models using HHT marginal power density, approximate entropy, and Fourier power density as the attributes.

TABLE I. THE IMPACT OF DIFFERENT ATTRIBUTE VECTORS ON THE ACCURACY OF SVM MODELS OF A REPRESENTATIVE PARTICIPANT

#	Attributes	Accuracy
1	α-original, β-original	85.25%
2	α-IMF4, β-IMF4	82.00%
3	α-IMF2, α-IMF3, α-IMF4, α-IMF5, β-IMF2, β-IMF3, β-IMF4, β-IMF5	88.00%
4	α-SE, β-SE	86.25%
5	α-original, β-original, α-SE, β-SE	87.50%
6	α-IMF2, α-IMF3, α-IMF4, α-IMF5, β-IMF2, β-IMF3, β-IMF4, β-IMF5, α-SE, β-SE	93.25%
7	α-IMF1, α-IMF2, α-IMF3, α-IMF4, α-IMF5, β-IMF1, β-IMF2, β-IMF3, β-IMF4, β-IMF5, α-SE, β-SE	91.25%
8	α-IMF2, α-IMF3, α-IMF4, α-IMF5, α-IMF6, β-IMF2, β-IMF3, β-IMF4, β-IMF5, β-IMF6, α-SE, β-SE	91.75%
9	α-IMF1, α-IMF2, α-IMF3, α-IMF4, α-IMF5, α-IMF6, β-IMF1, β-IMF2, β-IMF3, β-IMF4, β-IMF5, β-IMF6, α-SE, β-SE	91.75%
10	α-IMF1, α-IMF2, α-IMF3, α-IMF4, α-IMF5, α-IMF6, α-IMF7, α-IMF8, β-IMF1, β-IMF2, β-IMF3, β-IMF4, β-IMF5, β-IMF6, β-IMF7, β-IMF8, α-SE, β-SE	91.75%

TABLE II. THE ACCURACY OF SVM MODELS OF 20 PARTICIPANTS USING ATTRIBUTES #6

Participant	Accuracy	Participant	Accuracy
1	77.75%	11	81.50%
2	86.75%	12	84.00%
3	81.00%	13	83.25%
4	85.50%	14	88.25%
5	89.75%	15	89.00%
6	77.25%	16	72.25%
7	77.00%	17	90.25%
8	93.50%	18	82.00%
9	89.75%	19	93.25%
10	81.25%	20	92.75%
		Average	84.80%

TABLE III. THE ACCURACY OF PREDICTIONS WITH INDEPENDENT TEST DATA

Participant	Accuracy	Participant	Accuracy
1	82.00%	11	78.00%
2	91.00%	12	80.00%
3	92.00%	13	79.00%
4	66.00%	14	91.00%
5	89.00%	15	96.00%
6	76.00%	16	77.00%
7	73.00%	17	86.00%
8	92.00%	18	82.00%
9	89.00%	19	92.00%
10	76.00%	20	91.00%
		Average	83.90%

References

1. Klimesch, W., Doppelmayr, M., Russegger, H., Pachinger, T., & Schwaiger, J. (1998). Induced alpha band power changes in the human EEG and attention. *Neuroscience Letters, 244*(2), 73-76.
2. Lubar, J. F., Swartwood, M. O., Swartwood, J. N., & O'Donnell, P. H. (1995). Evaluation of the effectiveness of EEG neurofeedback training for ADHD in a clinical setting as measured by changes in TOVA scores, behavioral ratings, and WISC-R performance. *Biofeedback and Self-regulation, 20*(1), 83-99.
3. Hillard, B., El-Baz, A. S., Sears, L., Tasman, A., & Sokhadze, E. M. (2013). Neurofeedback Training Aimed to Improve Focused Attention and Alertness in Children With ADHD: A Study of Relative Power of EEG Rhythms Using Custom-Made Software Application. *Clinical Eeg and Neuroscience, 44*(3), 193-202.
4. Li, Y., Li, X., Ratcliffe, M., Liu, L., Qi, Y., & Liu, Q. A real-time EEG-based BCI system for attention recognition in ubiquitous environment. In *Proceedings of 2011 international workshop on Ubiquitous affective awareness and intelligent interaction, 2011* (pp. 33-40): ACM.
5. Liu, N.-H., Chiang, C.-Y., & Chu, H.-C. (2013). Recognizing the degree of human attention using EEG signals from mobile sensors. *Sensors, 13*(8), 10273-10286.
6. Xu, L., Liu, J., Xiao, G., & Jin, W. Characterization and classification of EEG attention based on fuzzy entropy. In *Third International Conference on Digital Manufacturing and Automation (ICDMA), 2012* (pp. 277-280): IEEE.
7. Hamadicharef, B., Zhang, H., Guan, C., Wang, C., Phua, K. S., Tee, K. P., et al. Learning EEG-based spectral-spatial patterns for attention level measurement. In *IEEE International Symposium on Circuits and Systems, 2009* (pp. 1465-1468): IEEE.
8. Lin, C.-F., & Zhu, J.-D. (2012). Hilbert-Huang transformation-based time-frequency analysis methods in biomedical signal applications. *Proceedings of the Institution of Mechanical Engineers Part H-Journal of Engineering in Medicine, 226*(H3), 208-216.
9. Wolpaw, J. R., Birbaumer, N., Heetderks, W. J., McFarland, D. J., Peckham, P. H., Schalk, G., et al. (2000). Brain-computer interface technology: A review of the first international meeting. *IEEE Transactions on Rehabilitation Engineering, 8*(2), 164-173.
10. K. I. Panoulas, Hadjileontiadis, L. J., & Panas, S. M. Hilbert-Huang Spectrum as a New Field for the Identification of EEG Event Related De-/Synchronization for BCI applications. In *30th Annual International Conference of the IEEE Engineering in Medicine and Biology Society, Vancouver, British Columbia, Canada, 2008*.
11. Li, S., Zhou, W., Yuan, Q., Geng, S., & Cai, D. (2013). Feature extraction and recognition of ictal EEG using EMD and SVM. *Computers in Biology and Medicine, 43*(7), 807-816.
12. Oweis, R. J., & Abdulhay, E. W. (2011). Seizure classification in EEG signals utilizing Hilbert-Huang transform. [journal article]. *BioMedical Engineering OnLine, 10*(1), 38.
13. Rehman, N., Xia, Y., & Mandic, D. P. Application of Multivariate empirical mode decomposition for seizure detection in EEG signals. In *Annual International Conference of the IEEE Engineering in Medicine and Biology, Buenos Aires, Argentina, 2010* (Vol. 1, pp. 1650-1653).
14. Shalbaf, R., Behnam, H., Sleigh, J. W., & Voss, L. J. (2012). Using the Hilbert-Huang transform to measure the electroencephalographic effect of propofol. *Physiological Measurement, 33*(2), 271-285.
15. Chen, S.-J., Peng, C.-J., Chen, Y.-C., Hwang, Y.-R., Lai, Y.-S., Fan, S.-Z., et al. (2016). Comparison of FFT and marginal spectra of EEG using empirical mode decomposition to monitor anesthesia. *Computer Methods and Programs in Biomedicine, 137*, 77-85.
16. Blankertz, B., Muller, K. R., Krusienski, D. J., Schalk, G., Wolpaw, J. R., Schlogl, A., et al. (2006). The BCI competition III: Validating alternative approaches to actual BCI problems. *IEEE Transactions on Neural Systems and Rehabilitation Engineering, 14*(2), 153-159.
17. Garrett, D., Peterson, D. A., Anderson, C. W., & Thaut, M. H. (2003). Comparison of linear, nonlinear, and feature selection methods for EEG signal classification. *IEEE Transactions on Neural Systems and Rehabilitation Engineering, 11*(2), 141-144.
18. Zhang, Y., Wei, S., Zhang, L., & Liu, C. (2018). Comparing the Performance of Random Forest, SVM and Their Variants for ECG Quality Assessment Combined with Nonlinear Features. *Journal of Medical and Biological Engineering*, 1-12.
19. Sałabun, W. (2014). Processing and spectral analysis of the raw EEG signal from the MindWave. *Przeglad Elektrotechniczny*(90), 169-174.
20. Jasper, H. H. (1958). Report of the committee on methods of clinical examination in electroencephalography. *Electroencephalography and Clinical Neurophysiology, 10*(2), 370-375.
21. Huang, N. E., Shen, Z., Long, S. R., Wu, M. C., Shih, H. H., Zheng, Q., et al. (1998). The empirical mode decomposition and the Hilbert spectrum for nonlinear and non-stationary time series analysis. *Proceedings of the Royal Society of London A: Mathematical, Physical and Engineering Sciences, 454*(1971), 903-995.

22. Boashash, B. (1992). Estimating and Interpreting the Instantaneous Frequency of a Signal-Part I: Fundamentals. *Proceedings of the IEEE, 80*(4), 520-538.
23. Bedrosian, E. (1963). A product theorem for Hilbert transforms. *Proceedings of the IEEE, 51*(5), 868-869.
24. Powell, G. E., & Percival, I. C. (1979). A spectral entropy method for distinguishing regular and irregular motion of Hamiltonian systems. *Journal of Physics A: Mathematical and General, 12*(11), 2053.
25. Humeau-Heurtier, A., Wu, C. W., Wu, S. D., Mah, G., & Abraham, P. (2016). Refined multiscale Hilbert-Huang spectral entropy and its application to central and peripheral cardiovascular data. *IEEE Transactions on Biomedical Engineering, 63*(11), 2405-2415.
26. Lotte, F., Congedo, M., Lecuyer, A., Lamarche, F., & Arnaldi, B. (2007). A review of classification algorithms for EEG-based brain-computer interfaces. *Journal of Neural Engineering, 4*(2), R1-R13.
27. Chang, C.-C., & Lin, C.-J. (2011). LIBSVM: a library for support vector machines. *ACM Transactions on Intelligent Systems and Technology (TIST), 2*(3), 27. Software available at http://www.csie.ntu.edu.tw/~cjlin/libsvm.
28. Kimeldorf, G., & Wahba, G. (1971). Some results on Tchebycheffian spline functions. *Journal of Mathematical Analysis and Applications, 33*(1), 82-95.
29. Sanchez, J. C., Carmena, J. M., Lebedev, M. A., Nicolelis, M. A. L., Harris, J. G., & Principe, J. C. (2004). Ascertaining the importance of neurons to develop better brain-machine interfaces. *IEEE Transactions on Biomedical Engineering, 51*(6), 943-953.